High-Speed Imaging Reveals Neurophysiological Links to Behavior in an Animal Model of Depression

Raag D. Airan, *et al.*

Science **317**, 819 (2007);
DOI: 10.1126/science.1144400

Science (print ISSN 0036-8075; online ISSN 1095-9203) is published weekly, except the last week in December, by the American Association for the Advancement of Science, 1200 New York Avenue NW, Washington, DC 20005.

regulatory omissions including Flo8 (not bound by either Ste12 or Tec1) and Mga1 (not bound by Ste12). Thus, although important differences can be found, TF binding to the promoters of other TFs was highly conserved between species relative to the level of conservation observed for other genes.

From those groups of genes that did not display conserved binding across the three species, one notable class was bound by Ste12 specifically in *S. mikatae* and *S. bayanus* and was enriched in genes involved in mating (GO category: "reproduction in single-celled organisms") in *S. cerevisiae* (Fig. 4, A and B). Unlike the gene targets in the diploid cells used in this study, these genes are targets of Ste12 in haploid *S. cerevisiae* cells (*20*, *21*), and this differential binding occurs despite the presence of conserved Ste12 binding motifs (fig. S3). Thus, Ste12 binding targets may be occupied under different conditions across related species. In *S. cerevisiae*, Ste12 binds to these sites only during mating, whereas in *S. mikatae* and *S. bayanus*, Ste12 binds to these same regions in diploid cells.

To extend this study outside of *Saccharomyces* yeasts, we also mapped the binding of the *Candida albicans* Ste12 ortholog, Cph1 (*22*). Cph1 functions in the dimorphic switch of this yeast, a process that shares many genetic components with pseudohyphal growth (*23*). A total of 52 significant Cph1 ChIP binding events (table S12) was detected under dimorphic growth conditions, with many residing upstream of known pathogenicity determinants (*24*–*27*). From these gene targets, 33 have recognizable orthologs in *S. cerevisiae*, and of these orthologs, 10, 10, and 13 displayed conserved binding with *S. cerevisiae*, *S. mikatae*, and *S. bayanus*, respectively. Although most gene targets of Cph1 in *C. albicans* are not conserved with the *Saccharomyces* species, the *C. albicans* orthologs bound by Ste12, like those from *S. mikatae* and *S. bayanus*, included a significant number of genes that function during reproduction and mating in *S. cerevisiae* ($P = 4 \times 10^{-3}$) (*18*). Thus, in *C. albicans*, like in *S. mikatae* and *S. bayanus*, the Ste12 ortholog also binds to genes required for mating in *S. cerevisiae* under filamentous growth conditions, raising the possibility that these genes have become more specialized in *S. cerevisiae*.

We find that extensive regulatory changes can exist in closely related species, which is consistent with a recent study that showed that distinct regulatory circuits can produce similar regulatory outcomes in *S. cerevisiae* and *C. albicans* (*28*). Furthermore, although *S. cerevisiae* and *S. mikatae* are quite similar to one another at the nucleotide sequence level, they are equally different to each other and to *S. bayanus* in their TF profiles. We expect that the extensive binding site differences observed in this study reflect the rapid specialization of these organisms for their distinct ecological environments and that differences in transcription regulation between related species may be responsible for rapid evolutionary adaptation to varied ecological niches.

References and Notes

1. P. Cliften *et al.*, *Science* **301**, 71 (2003).
2. M. Kellis, N. Patterson, M. Endrizzi, B. Birren, E. S. Lander, *Nature* **423**, 241 (2003).
3. M. Tompa *et al.*, *Nat. Biotechnol.* **23**, 137 (2005).
4. V. R. Iyer *et al.*, *Nature* **409**, 533 (2001).
5. B. Ren *et al.*, *Science* **290**, 2306 (2000).
6. J. Piskur, R. B. Langkjaer, *Mol. Microbiol.* **53**, 381 (2004).
7. H. D. Madhani, G. R. Fink, *Science* **275**, 1314 (1997).
8. V. Gavrias, A. Andrianopoulos, C. J. Gimeno, W. E. Timberlake, *Mol. Microbiol.* **19**, 1255 (1996).
9. H. Liu, C. A. Styles, G. R. Fink, *Science* **262**, 1741 (1993).
10. S. Fields, I. Herskowitz, *Cell* **42**, 923 (1985).
11. A. R. Borneman *et al.*, *Funct. Integr. Genomics*, in press; preprint available at www.springerlink.com/content/w65529354201666h/.
12. See supporting material on *Science* Online.
13. X. S. Liu, D. L. Brutlag, J. S. Liu, *Nat. Biotechnol.* **20**, 835 (2002).
14. J. W. Dolan, C. Kirkman, S. Fields, *Proc. Natl. Acad. Sci. U.S.A.* **86**, 5703 (1989).
15. T. L. Bailey, M. Gribskov, *Bioinformatics* **14**, 48 (1998).
16. S. Chou, S. Lane, H. Liu, *Mol. Cell. Biol.* **26**, 4794 (2006).
17. S. Prinz *et al.*, *Genome Res.* **14**, 380 (2004).
18. E. I. Boyle *et al.*, *Bioinformatics* **20**, 3710 (2004).
19. A. R. Borneman *et al.*, *Genes Dev.* **20**, 435 (2006).
20. C. T. Harbison *et al.*, *Nature* **431**, 99 (2004).
21. J. Zeitlinger *et al.*, *Cell* **113**, 395 (2003).
22. T. Jones *et al.*, *Proc. Natl. Acad. Sci. U.S.A.* **101**, 7329 (2004).
23. C. Sanchez-Martinez, J. Perez-Martin, *Curr. Opin. Microbiol.* **4**, 214 (2001).
24. C. E. Birse, M. Y. Irwin, W. A. Fonzi, P. S. Sypherd, *Infect. Immun.* **61**, 3648 (1993).
25. B. R. Braun, W. S. Head, M. X. Wang, A. D. Johnson, *Genetics* **156**, 31 (2000).
26. B. R. Braun, A. D. Johnson, *Genetics* **155**, 57 (2000).
27. T. C. White, S. H. Miyasaki, N. Agabian, *J. Bacteriol.* **175**, 6126 (1993).
28. A. E. Tsong, B. B. Tuch, H. Li, A. D. Johnson, *Nature* **443**, 415 (2006).

29. The authors would like to thank P. Chambers and D. Gelperin for comments on the manuscript. Funding was provided by NIH grants (to M.S. and M.G.) and by the Burroughs Wellcome Foundation. Detailed lists of binding regions, conservation information, and motif scores are available from www.gersteinlab.org/proj/regnetdiverge.

Supporting Online Material

www.sciencemag.org/cgi/content/full/317/5839/815/DC1
Materials and Methods
Fig. S1 to S5
Tables S1 to S14
References

2 February 2007; accepted 20 June 2007
10.1126/science.1140748

High-Speed Imaging Reveals Neurophysiological Links to Behavior in an Animal Model of Depression

Raag D. Airan,[1]* Leslie A. Meltzer,[2]* Madhuri Roy,[1] Yuqing Gong,[3,4] Han Chen,[3] Karl Deisseroth[1,5]†

The hippocampus is one of several brain areas thought to play a central role in affective behaviors, but the underlying local network dynamics are not understood. We used quantitative voltage-sensitive dye imaging to probe hippocampal dynamics with millisecond resolution in brain slices after bidirectional modulation of affective state in rat models of depression. We found that a simple measure of real-time activity—stimulus-evoked percolation of activity through the dentate gyrus relative to the hippocampal output subfield—accounted for induced changes in animal behavior independent of the underlying mechanism of action of the treatments. Our results define a circuit-level neurophysiological endophenotype for affective behavior and suggest an approach to understanding circuit-level substrates underlying psychiatric disease symptoms.

The hippocampus, as an integral component of the limbic system, is a focus of depression research (*1*), drives other brain regions implicated in depression, and appears to serve as a primary site of action for antidepressants that inhibit pathological hyperactivity (*2*, *3*). Complicating this picture, however, is evidence suggesting that antidepressants can stimulate hippocampal activity. Antidepressant-induced hippocampal neurogenesis is linked to behavioral responses (*4*, *5*); moreover, excitatory hippocampal neurons are injured by chronic stress (*6*, *7*). Animal models have proven useful in identifying molecular and cellular markers relevant to depression (*8*–*10*) but have not identified neurophysiological final common pathways relevant to behavior. Voltage-sensitive dye imaging (VSDI) could allow analysis of disease-related neural activity on millisecond time scales, with micrometer spatial resolution and a scope spanning entire brain networks (*11*). We applied VSDI to hippocampal physiology in the chronic mild stress (CMS) model, a well-validated rodent

[1]Department of Bioengineering, Stanford University, Stanford, CA 94305, USA. [2]Neuroscience Program, Stanford University, Stanford, CA 94305, USA. [3]Department of Electrical Engineering, Stanford University, Stanford, CA 94305, USA. [4]Department of Statistics, Stanford University, Stanford, CA 94305, USA. [5]Department of Psychiatry and Behavioral Sciences, Stanford University, Stanford, CA 94305, USA.

*These authors contributed equally to this work.
†To whom correspondence should be addressed. E-mail: deissero@stanford.edu

model of core depressive behavioral symptoms (*12*).

Evoked activity was recorded with VSDI in acute horizontal slices prepared from the ventral hippocampus of adult rats (Fig. 1A) (*13*, *14*). Signals reflecting local neuronal network activity were extinguished by 2,3-dihydroxy-6-nitro-7-sulfamoylbenzo[*f*]quinoxaline-2,3-dione (NBQX) and D-2-amino-5-phosphonopentanoic acid (D-AP5) and therefore required excitatory transmission (Fig. 1B). We used cross-correlation to extract reliable, quantitative features of the network response (Fig. 1, C and D, and figs. S1 and S2), computing the maximal response amplitude of each pixel (Fig. 1D, top right, and fig. S3, right) and the time at which this maximal amplitude occurred ("phase"; Fig. 1D, top left, and fig. S3, left). In our experiments, phase distributions were independent of treatment group and coherent in the region responding to stimulation, which was isolated computationally in blinded analysis (Fig. 1D, bottom, and figs. S4 to S6). A simple metric of circuit response ("total activity," defined as the mean amplitude multiplied by the area of the calculated region of interest) (*13*) was found to be linear in this stimulus range and reliable across slices (Fig. 2B).

To quantify behaviorally relevant hippocampal dynamics in a rodent model, we applied CMS (Fig. 2A, left) or delivered one of two chronic antidepressant treatments: the selective serotonin reuptake inhibitor fluoxetine or the tricyclic antidepressant imipramine (the typical antipsychotic haloperidol served as a pharmacological control; Fig. 2A, right). Depression-like behavior was quantified, blind to treatment condition, in terms

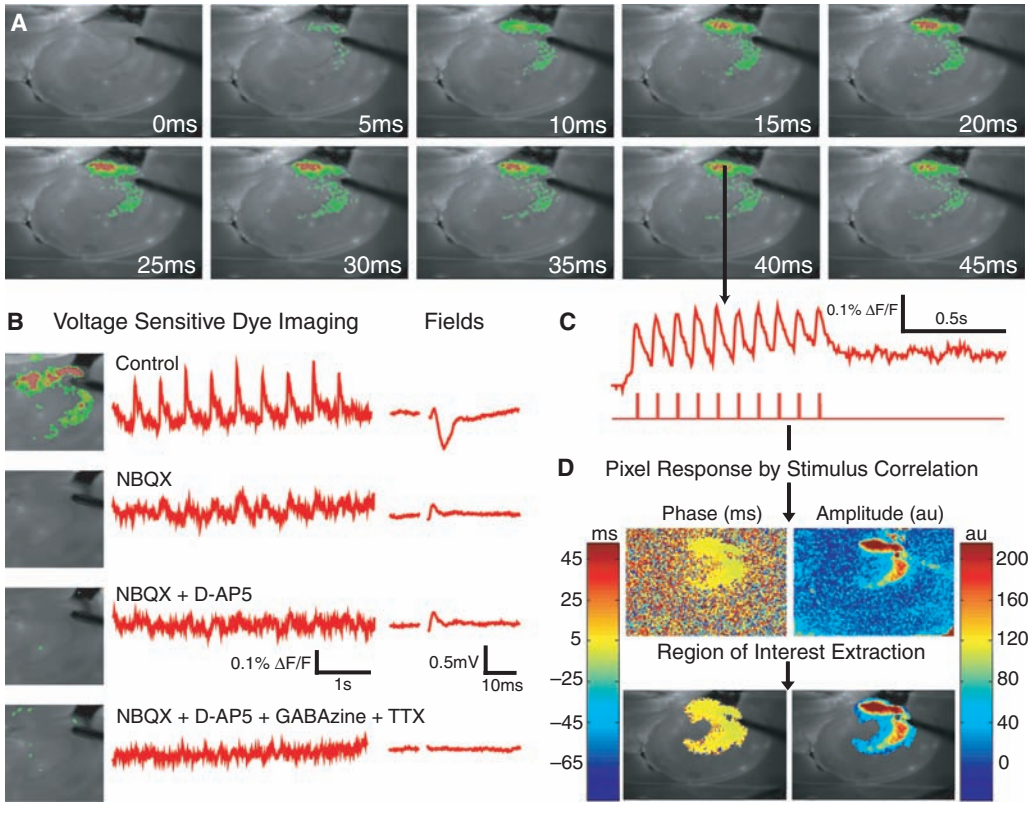

Fig. 1. Voltage-sensitive dye imaging (VSDI) of hippocampal network activity. (**A**) Representative filmstrip acquired using VSDI. Elapsed times are relative to a single stimulus pulse applied to DG; warmer colors indicate greater activity (relative change in VSD fluorescence, $\Delta F/F$). Data represent the average of four individual acquisitions. (**B**) VSDI signal is abolished by blockers of excitatory synaptic transmission (10 μM NBQX and 25 μM D-AP5). GABAzine (20 μM) and tetrodotoxin (TTX, 1 μM) application subsequently confirmed signal extinction. (**C**) Single-pixel response ($\Delta F/F$ versus time; top) from the indicated region to the given stimulus train (bottom). (**D**) Phase (top left) and amplitude (top right) of maximal correlation between the stimulus and response at each pixel. The synchronously responding region was extracted computationally, with the same phase criteria applied to all treatment groups, on the basis of similar phase values of responding pixels (bottom); au, arbitrary units.

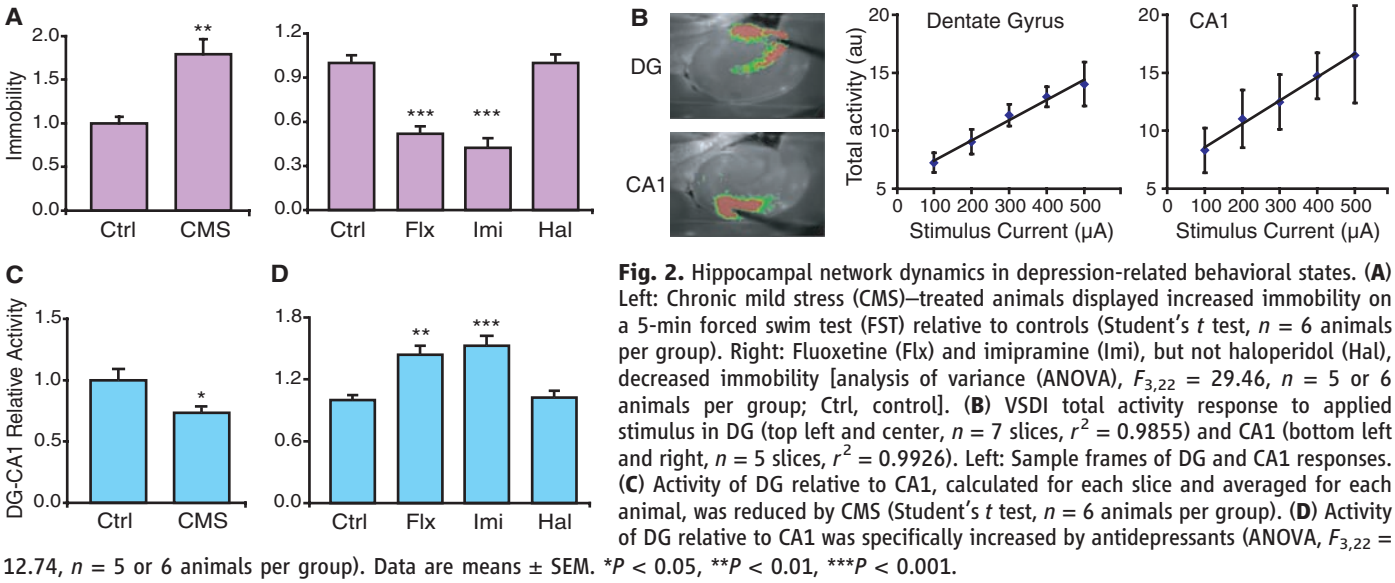

Fig. 2. Hippocampal network dynamics in depression-related behavioral states. (**A**) Left: Chronic mild stress (CMS)–treated animals displayed increased immobility on a 5-min forced swim test (FST) relative to controls (Student's *t* test, $n = 6$ animals per group). Right: Fluoxetine (Flx) and imipramine (Imi), but not haloperidol (Hal), decreased immobility [analysis of variance (ANOVA), $F_{3,22} = 29.46$, $n = 5$ or 6 animals per group; Ctrl, control]. (**B**) VSDI total activity response to applied stimulus in DG (top left and center, $n = 7$ slices, $r^2 = 0.9855$) and CA1 (bottom left and right, $n = 5$ slices, $r^2 = 0.9926$). Left: Sample frames of DG and CA1 responses. (**C**) Activity of DG relative to CA1, calculated for each slice and averaged for each animal, was reduced by CMS (Student's *t* test, $n = 6$ animals per group). (**D**) Activity of DG relative to CA1 was specifically increased by antidepressants (ANOVA, $F_{3,22} = 12.74$, $n = 5$ or 6 animals per group). Data are means ± SEM. $^*P < 0.05$, $^{**}P < 0.01$, $^{***}P < 0.001$.

of immobility on the forced swim test (FST); in this test, immobility is increased by CMS and decreased by antidepressants (*15*). In all drug experiments, a 48-hour delay between the last dose and behavioral assessment excluded acute drug effects on behavior that do not have relevant clinical correlates (*16*). Relative to controls, CMS animals were more immobile over a 5-min FST, indicating a depressed-like state (Fig. 2A, left), whereas antidepressant-treated but not antipsychotic-treated animals showed less immobility (Fig. 2A, right).

We then conducted VSDI of evoked activity in ventral hippocampal slices (*14*) from these animals; blind to treatment condition, we probed both the dentate gyrus (DG) and CA1, hypothesizing different effects in the input and output hippocampal subfields (*17*–*20*). We found that activity propagation in DG relative to CA1 provided the most reliable predictor of FST performance on an animal-by-animal basis (Fig. 2C). DG activity was reduced in CMS-treated animals (fig. S7A), whereas CA1 activity was increased (fig. S7B); the CA1 contribution is compatible with results linking depression to elevated hippocampal output (*2*, *3*, *21*), and the DG contribution is consistent with data suggesting reduced hippocampal activity in depression (*4*, *6*).

We found the opposite pattern in antidepressant-treated animals (Fig. 2D and fig. S7), with increased activity propagation in DG (fig. S7C) and reduced activity in CA1 (fig. S7D). These effects were specific to antidepressants; antipsychotic treatment showed no effect on either subfield (fig. S7, C and D). Again, the activity propagation in DG relative to CA1 provided the most reliable (across-individual) indicator of the behavioral phenotype (Fig. 2D; $r^2 = 0.5251$, $P < 10^{-6}$, across CMS and drug groups).

To model clinical use of antidepressants, we next concomitantly administered fluoxetine during the last 2 weeks of 5-week CMS (Fig. 3). FST blinded to treatment condition confirmed that fluoxetine treatment reversed the behavioral effects of CMS (Fig. 3A), and VSDI demonstrated that the activity propagation in DG relative to CA1 significantly accounted for this effect (Fig. 3, B and C). On an individual-animal basis, this measure of activity propagation on the millisecond time scale regressed linearly with the FST scores and explained more than half of the bidirectional behavioral variation (Fig. 3C; $r^2 = 0.5545$, $P < 10^{-6}$) across all four independent treatment arms. Open-field tests (OFTs) from the same animals provided a test of the specificity of the network dynamics phenotype. We observed no significant differences between groups in locomotion or anxiety-related behavior on the OFT (Fig. 3, D and E), and there was no correlation between VSDI physiology and OFT scores (Fig. 3F; $r^2 = 0.0306$, $P > 0.4$), indicating specificity for depression-relevant behavior.

To address the cellular mechanism, we next probed for changes in hippocampal neurogenesis—hypothesized to be relevant to depression [(*4*, *5*), but see (*22*)]—in the same animals represented in Fig. 3. In accord with previous observations (*4*, *5*), fluoxetine increased both the number and density of newborn neurons [as assessed by blinded, unbiased stereology of cells positive for 5-bromo-2′-deoxyuridine (BrdU) and Doublecortin (Dcx; immature neuronal marker)] (*13*) in the ventral DG, both in the presence and absence of CMS (Fig. 4, A and B), whereas CMS alone did not significantly alter the production (Fig. 4, A and B) of new neurons despite behavioral and circuit dynamics effects in the same animals (Fig. 3, A to C). Similarly effective CMS did not affect the survival of newborn neurons (Fig. 2 and fig. S12). These data indicate that circuit dynamics changes can account for bidirectional affective state modulation despite fundamental differences in cellular processes occurring during depressed-like state induction and treatment.

To test the capability of a temporally defined cohort of new neurons to modulate behavior and circuit dynamics, we treated animals for 1 week with fluoxetine to up-regulate neurogenesis, followed by a 3-week delay to permit functional integration of neurons born during treatment

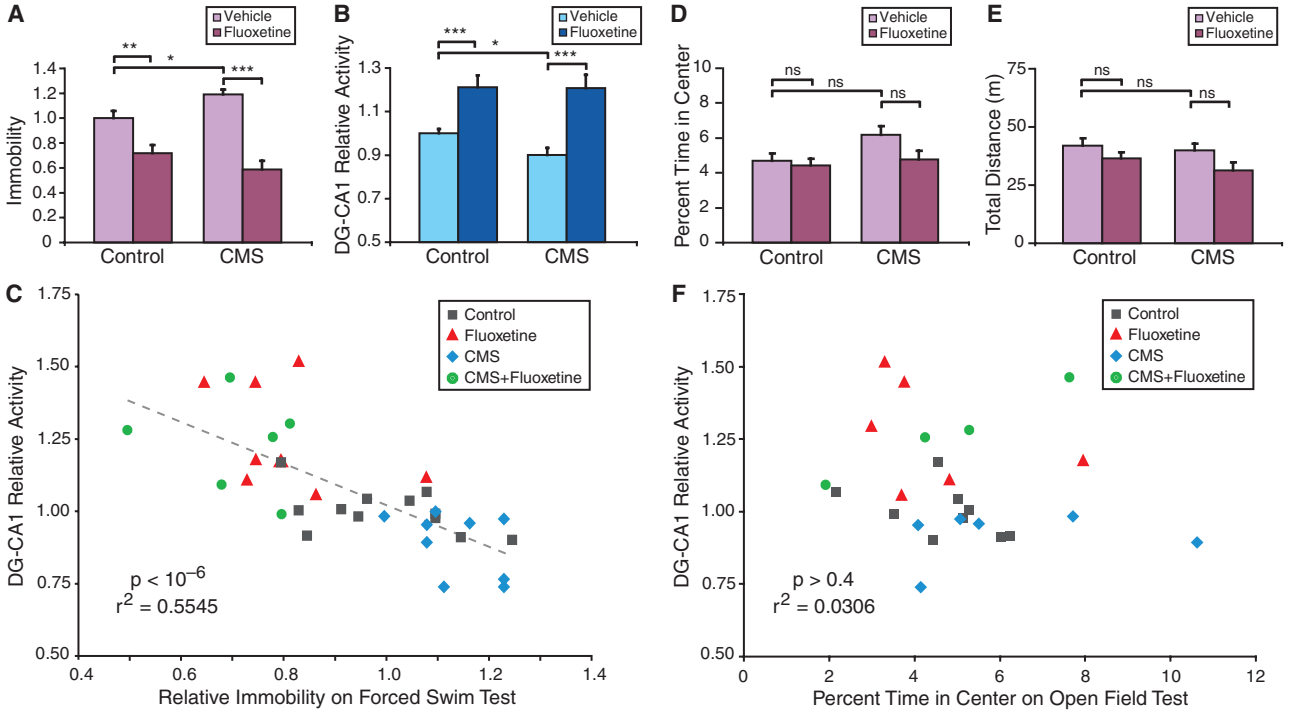

Fig. 3. Hippocampal network dynamics predict antidepressant treatment of depressed-like states. Fluoxetine was concomitantly administered during the last 2 weeks of 5-week CMS. (**A**) CMS increased immobility and fluoxetine decreased immobility in both control and CMS groups (ANOVA, $F_{3,34} = 19.24$, $n = 8$ to 12 animals per group). (**B**) Activity of DG relative to CA1 was decreased in CMS animals and was increased by fluoxetine (ANOVA, $F_{3,34} = 16.17$, $n = 6$ to 12 animals per group). (**C**) Linear regression of activity of DG relative to CA1 against FST scores for each individual animal ($r^2 = 0.5545$, $P < 10^{-6}$, $n = 35$ individual animals). (**D** and **E**) On the open-field test (OFT), no differences were observed in percent time in center [(D); ANOVA, $F_{3,20} = 1.021$, $P > 0.05$, $n = 4$ to 9 animals per group] or total distance [(E); ANOVA, $F_{3,20} = 1.776$, $P > 0.05$, $n = 4$ to 9 animals per group]. (**F**) Linear regression of activity of DG relative to CA1 against percent time in center for each individual animal ($r^2 = 0.0306$, $P > 0.4$, $n = 25$ individual animals).

(Fig. 4C). In some animals, we ablated hippocampal neurogenesis via irradiation (10 Gy/day for 2 days) 1 month before drug exposure; control experiments revealed no effect of irradiation alone on excitability, network dynamics, or behavior on this time scale (Fig. 4E and figs. S8 and S11). The fluoxetine pulse gave rise to a temporally defined cohort of new neurons (Fig. 4D and figs. S13 and S14) and reduced FST immobility in a manner blocked by irradiation (Fig. 4E, top), indicating that increased neurogenesis indeed is required for these antidepressant behavioral effects (*5*). However, irradiation alone did not affect behavior (Fig. 4E, top); therefore, inhibition of neurogenesis is neither sufficient (Fig. 4E, top) nor necessary (Fig. 2A, left; Fig. 3A; Fig. 4, A and B; and fig. S12) to induce a depressed-like state.

To quantitatively explore circuit dynamics modulation by the temporally defined cohort of new neurons, we conducted VSDI in the ventral hippocampus from these animals. The activity propagation in DG relative to CA1 was indeed increased (Fig. 4E, bottom), and only the DG effect was neurogenesis-dependent (fig. S8, A and B). Although it may be counterintuitive that a small number of new neurons (*23*) could affect circuit dynamics, simple modeling predicted that rare new neurons can increase the recruited active network area (fig. S9). We therefore analyzed VSDI signal components (area and amplitude) to determine their contribution to the observed changes in DG physiology, and found that the circuit-level effect of a temporally defined cohort of fluoxetine-induced newborn neurons on DG activity is indeed due primarily to increased active DG area (fig. S8), a parameter readily detectable by high-speed VSDI as demonstrated here.

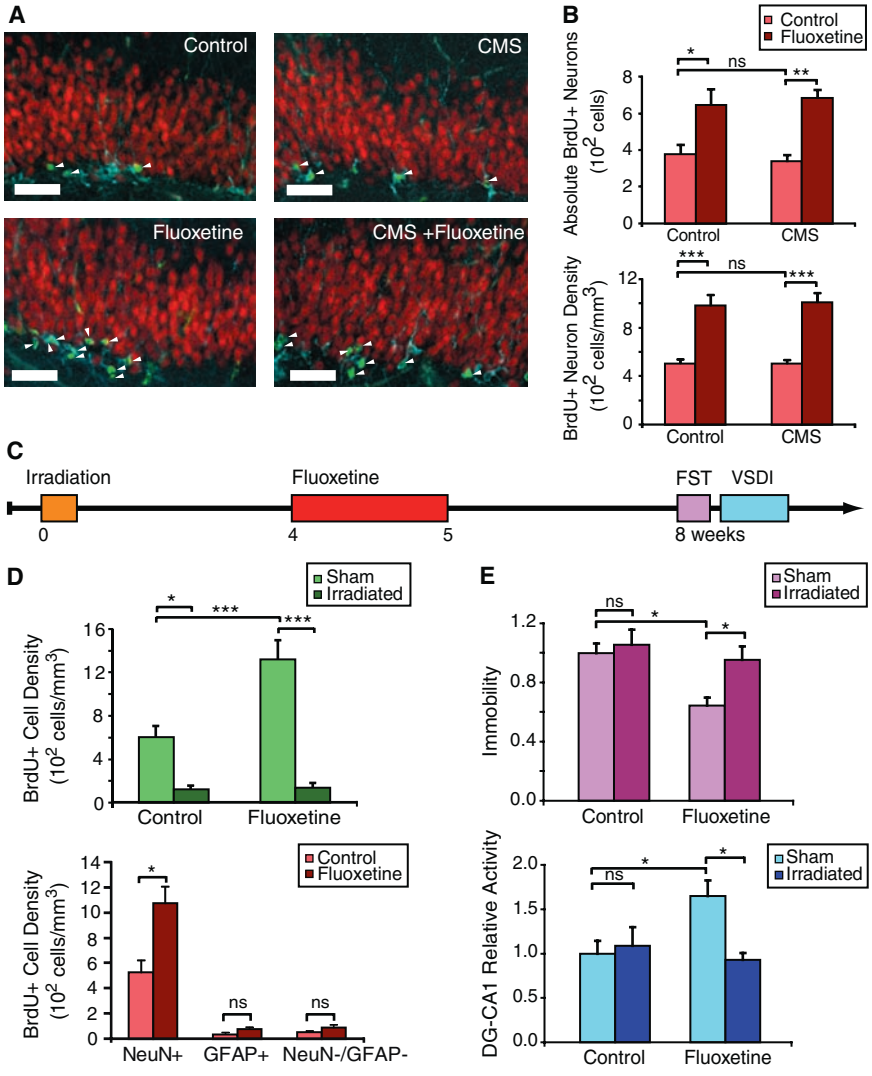

Fig. 4. VSDI resolution of neurogenesis-dependent circuit dynamics changes underlying antidepressant response. (**A**) Representative confocal DG images labeled for BrdU (green), NeuN (mature neuronal marker, red), and Dcx (immature neuronal marker, cyan). Arrowheads indicate $BrdU^+$ neurons. Scale bar, 50 μm. (**B**) New neuron ($BrdU^+/Dcx^+$) counts (top) and density (bottom) in ventral hippocampus (same animals as in Fig. 3) were increased with fluoxetine treatment but unchanged with CMS (counts: ANOVA, $F_{3,27} = 9.670$; density: $F_{3,27} = 20.68$; $n = 6$ to 8 animals per group). (**C**) One month after irradiation designed to ablate hippocampal neurogenesis, fluoxetine or vehicle was administered for 1 week, followed by a 3-week delay for newborn neuron incorporation. (**D**) Top: $BrdU^+$ cell density was increased after fluoxetine treatment and substantially decreased with irradiation (ANOVA, $F_{3,24} = 29.72$, $n = 4$ to 8 animals per group). Bottom: Fluoxetine treatment specifically increased the density of newborn neurons ($BrdU^+/NeuN^+$) in DG [glial fibrillary acidic protein (GFAP), astrocytic marker; Student's t test, $n = 6$ animals per group]. (**E**) Top: Fluoxetine-treated animals showed decreased FST immobility; no effects were observed with irradiation (ANOVA, $F_{3,23} = 7.757$, $n = 6$ animals per group). Bottom: Irradiation blocked increased activity of DG relative to CA1 after fluoxetine treatment (ANOVA, $F_{3,22} = 3.997$, $n = 5$ or 6 animals per group).

These data suggest that behavioral changes can be linked to a common network dynamics phenotype without requiring a common etiology or mechanism such as neurogenesis. Indeed, we propose that genetic or environmental factors with diverse cellular mechanisms (*4*–*7*, *17*, *18*, *24*) that are operative in different individuals may exert behavioral effects through a common activity-percolation phenotype. Although many antidepressants are associated with increased seizure risk and therefore could involve increased activity propagation through the DG, other antidepressant treatments clearly do not directly target the hippocampus, such as deep brain stimulation (DBS), which typically targets Cg25 or the nucleus accumbens. However, DBS reduces activity in Cg25 (*25*), which receives excitatory drive from the hippocampus (*2*, *3*, *21*), suggesting that Cg25 DBS can intervene downstream of an overactive CA1. There had been no obvious way to unify into a single model the hippocampal atrophy seen in depression (*7*, *24*) with the likely increased excitatory drive from hippocampus to cortex associated with depression (*2*, *25*). Our results suggest that the increased subgenual cingulate activity in depression could result in part from increased CA1 activity, whereas the reduced intrinsic hippocampal function observed in depression is consistent with decreased DG activity.

Hippocampal dysfunction related to mood may be experienced cognitively [e.g., as hopelessness (*26*)], which can manifest clinically as patients' inability to foresee or navigate a reasonable and hopeful plan within the environment. Theoretical models of the dorsal hippocampus have described comparative interactions between DG and CA1 (*19*, *20*) in which CA1 activity indicates discrepancies between predictive information from DG and sensory information from the cortex. Depression therefore could be associated with the failure to predict, navigate through, or adapt to environmental changes (experienced as hopelessness) resulting from failed ventral DG associative/predictive activity or increased error signals from CA1. If that is the case, the intensity of the resulting dysphoria may be modulated by anxiety or reward pathways (amygdala, nucleus accumbens, and mesolimbic dopamine projections) or the prefrontal and cingulate cortices (*27*). Indeed, identification of this hippocampal neurophysiological endophenotype may serve as a

starting point in mapping the network-level changes in other brain regions implicated in depression. High-speed, circuit-level optical methods are better suited than single-cell physiology to detect and quantitatively describe spatiotemporal dynamics (such as areal spread of activity) that may be altered in psychiatric disease. These circuit dynamics measures relate to how information propagates rather than to a specific neural code. We propose that depression may depend on changes in the ability of information representations to organize and percolate through sparsely active networks.

References and Notes

1. S. Campbell, G. Macqueen, *J. Psychiatry Neurosci.* **29**, 417 (2004).
2. H. S. Mayberg *et al.*, *Biol. Psychiatry* **48**, 830 (2000).
3. D. A. Seminowicz *et al.*, *Neuroimage* **22**, 409 (2004).
4. J. L. Warner-Schmidt, R. S. Duman, *Hippocampus* **16**, 239 (2006).
5. L. Santarelli *et al.*, *Science* **301**, 805 (2003).
6. C. Mirescu, E. Gould, *Hippocampus* **16**, 233 (2006).
7. R. M. Sapolsky, *Arch. Gen. Psychiatry* **57**, 925 (2000).
8. L. H. Tecott, E. J. Nestler, *Nat. Neurosci.* **7**, 462 (2004).
9. W. M. Cowan, D. H. Harter, E. R. Kandel, *Annu. Rev. Neurosci.* **23**, 343 (2000).
10. J. F. Cryan, A. Holmes, *Nat. Rev. Drug Discov.* **4**, 775 (2005).
11. A. Grinvald, R. Hildesheim, *Nat. Rev. Neurosci.* **5**, 874 (2004).
12. P. Willner, *Neuropsychobiology* **52**, 90 (2005).
13. See supporting material on *Science* Online.
14. D. M. Bannerman *et al.*, *Neurosci. Biobehav. Rev.* **28**, 273 (2004).
15. J. F. Cryan, R. J. Valentino, I. Lucki, *Neurosci. Biobehav. Rev.* **29**, 547 (2005).
16. C. López-Rubalcalva, I. Lucki, *Neuropsychopharmacology* **22**, 191 (2000).
17. S. G. Walling, C. W. Harley, *J. Neurosci.* **24**, 598 (2004).
18. S. Birnstiel, T. J. List, S. G. Beck, *Synapse* **20**, 117 (1995).
19. J. E. Lisman, A. A. Grace, *Neuron* **46**, 703 (2005).
20. M. E. Hasselmo, H. Eichenbaum, *Neural Netw.* **18**, 1172 (2005).
21. H. S. Mayberg *et al.*, *Am. J. Psychiatry* **156**, 675 (1999).
22. F. A. Henn, B. Vollmayr, *Biol. Psychiatry* **56**, 146 (2004).
23. H. A. Cameron, R. D. G. McKay, *J. Comp. Neurol.* **435**, 406 (2001).
24. B. S. McEwen, *Annu. Rev. Neurosci.* **22**, 105 (1999).
25. H. S. Mayberg *et al.*, *Neuron* **45**, 651 (2005).
26. E. J. Nestler *et al.*, *Neuron* **34**, 13 (2002).
27. W. C. Drevets, *Curr. Opin. Neurobiol.* **11**, 240 (2001).

28. We thank the Deisseroth lab, J. R. Huguenard, T. D. Palmer, R. C. Malenka, and B. K. Ormerod for helpful discussions. Supported by the National Institute on Drug Abuse, the National Institute of Mental Health, the NIH Director's Pioneer Award, NARSAD, the American Psychiatric Institute for Research and Education, and the Snyder, Culpeper, Coulter, Klingenstein, Whitehall, McKnight, and Albert Yu and Mary Bechmann Foundations (K.D.); the Stanford Medical Scientist Training Program (R.D.A.); and a Stanford Bio-X predoctoral fellowship (L.A.M.).

Supporting Online Material

www.sciencemag.org/cgi/content/full/1144400/DC1
Materials and Methods
Figs. S1 to S14
References

30 April 2007; accepted 28 June 2007
Published online 5 July 2007;
10.1126/science.1144400
Include this information when citing this paper.

Characterizing the Limits of Human Visual Awareness

Liqiang Huang,[1]* Anne Treisman,[1] Harold Pashler[2]

Momentary awareness of a visual scene is very limited; however, this limitation has not been formally characterized. We test the hypothesis that awareness reflects a surprisingly impoverished data structure called a labeled Boolean map, defined as a linkage of just one feature value per dimension (for example, the color is green and the motion is rightward) with a spatial pattern. Features compete with each other, whereas multiple locations form a spatial pattern and thus do not compete. Perception of the colors of two objects was significantly improved by successive compared with simultaneous presentation, whereas perception of their locations was not. Moreover, advance information about which objects are relevant aided perception of colors much more than perception of locations. Both results support the Boolean map hypothesis.

Many experiments have explored the process of attentional selection in vision, chiefly through visual search tasks in which observers try to find a single specified target, which may or may not be present in a display (*1*–*4*). Selection sometimes involves sequential checking of different elements, whereas in other search tasks a parallel selection process can exclude all but a single target (*3*, *5*). What has been scarcely investigated at all, however, is an even more fundamental question about human vision: What is the informational content of any single momentary act of conscious perception?

Consider, for example, the array of four colored disks shown in Fig. 1A. Can a human observer attend to all four disks and simultaneously be aware of the presence of two blue, one red, and one green disk? A recently proposed theory of attention contends that we cannot (*6*). According to this account, momentary conscious access, although flexibly controlled through voluntary attending, is nonetheless constrained to have the representational content of a data structure termed a labeled Boolean map. There is evidence that visual perception analyzes the scene along a number of different basic dimensions, such as color, motion, spatial frequency, and orientation (*3*, *5*, *7*). The data structure of a labeled Boolean map may thus associate at most one value at a time for each of these independent visual dimensions (for example, color is green and motion is rightward) as labels with a spatial pattern (i.e., the set of location values composing the Boolean map) (*6*). Here, we deal only with the case of within-dimension competition, so the claim can be abbreviated for present purposes as awareness of only a single feature value. A choice of three potential Boolean maps could represent either the red, the green, or the blue disk(s) in Fig. 1A. These would afford the observer conscious access to both the location(s) and the color of the attended disk(s). On the other hand, the map could instead encompass disks of more than one color simultaneously, and in that case there would be explicit awareness of all locations but not of the colors. Figure 1B illustrates the representational content of a few (but not all) of the possible percepts that might be elicited by these stimuli according to the present hypothesis.

The claim that conscious access is limited to a "one-feature-multiple-locations" format generates numerous predictions (*6*). Here, we focus on one especially critical and counterintuitive prediction, namely the proposed asymmetry between conscious access to multiple features and to multiple locations. The Boolean map theory predicts that multiple features can only be consciously accessed one by one, whereas multiple locations can be accessed at the same time.

In the first experiment, we presented two objects either at the same time (simultaneous condition) or one by one (successive condition), followed by a single probe (either a color patch or a location marker, to be judged as having been present in the display or not). For any type of visual information (feature or location), if two such values cannot be accessed at the same time, then observers should perform worse in the simultaneous condition. If, however, two such values can be simultaneously accessed without attentional limitation, then observers should perform equally in

[1]Center for the Study of Brain, Mind, and Behavior, Princeton University, Princeton, NJ 08544, USA. [2]Department of Psychology, University of California, San Diego, La Jolla, CA 92093, USA.

*Present address: Department of Psychology, Chinese University of Hong Kong, Shatin, NT, Hong Kong, China. To whom correspondence should be addressed. E-mail: lqhuang@psy.cuhk.edu.hk